

# Biodegradable silicon nanoneedles delivering nucleic acids intracellularly induce localized *in vivo* neovascularization

C. Chiappini<sup>1,†</sup>, E. De Rosa<sup>2,†</sup>, J. O. Martinez<sup>2</sup>, X.W. Liu<sup>2</sup>, J. Steele<sup>1</sup>, M.M. Stevens<sup>1,3</sup>,

§\*, E. Tasciotti<sup>2,§,\*</sup>

+ These authors contributed equally to this work

§ These authors contributed equally to this work

\*To whom correspondence should be addressed:

Dr. Ennio Tasciotti

Department of Nanomedicine, Houston Methodist Research Institute

6670 Bertner Ave, Houston, TX, 77030

Tel: +1 713-441-7319

[etasciotti@houstonmethodist.org](mailto:etasciotti@houstonmethodist.org)

Professor Molly Stevens

Department of Materials, Department of Bioengineering and Institute of

Biomedical Engineering

Imperial College London

SW7 2AZ

Tel: +44 (0)20 7594 6804

[m.stevens@imperial.ac.uk](mailto:m.stevens@imperial.ac.uk)

1. Department of Materials, Imperial College London, London, SW6 7PB, UK

2. Department of Nanomedicine, Houston Methodist Research Institute, Houston, Texas 77030, USA

3. Department of Bioengineering and Institute of Biomedical Engineering, Imperial College London, London, SW6 7PB, UK



# Supplementary Information

## Table of Contents

<b>Supplementary Information .....</b>	<b>5</b>
Calculation of porous silicon nanoneedles force to failure .....	5
Estimation of force necessary for penetration .....	5
Efficient loading and sustained release of nucleic acids. ....	5
<b>Supplementary Figures .....</b>	<b>7</b>
<b>Supplementary Movie Captions.....</b>	<b>24</b>
<b>Materials and Methods .....</b>	<b>25</b>
Patterning of Si wafers.....	25
Synthesis of nanoneedles by metal assisted chemical etch.....	25
Controlling Nanoneedles' Porosity.....	25
Controlling Nanoneedles' Diameter.....	25
Mechanical testing of Nanoneedles.....	26
Cell Culture.....	26
Nanoinjection: Nanoneedles on bottom .....	26
Nanoinjection: Nanoneedles on top .....	26
MTT Assay .....	26
LDH Assay .....	27
SEM analysis of nanoneedles interfacing.....	27
SEM/FIB cross sectional analysis of nanoneedles interfacing .....	27
Confocal Microscopy of nanoneedles interfacing .....	27
ICP-AES .....	28
siRNA loading.....	28
siRNA release .....	28
siRNA delivery <i>in vitro</i> .....	28
In-cell western for GAPDH silencing.....	29
siRNA and GFP plasmid loading, delivery and expression <i>in vitro</i> .....	29
Nanoneedles treatment <i>in vivo</i> .....	29
RT-PCR analysis of plasmid VEGF delivery.....	30
Live animal imaging and quantification .....	30
Intravital animal confocal microscopy .....	31
H&E Histology .....	31
Transmission Electron Microscopy <i>in vivo</i> .....	31
<b>References.....</b>	<b>33</b>

## Supplementary Information

### Calculation of porous silicon nanoneedles force to failure

It is possible to estimate the force to failure for conical needles where a force is applied to the tip, by deriving appropriate calculations from existing models<sup>1,2</sup>. Because porous silicon is a brittle material, the yield to failure is equal to the yield strength  $Y_s$  (100MPa)<sup>3</sup>. To evaluate the failure load  $P_t$  it suffices to solve the following equation for  $P_t$

$$Y_s = \frac{P_t}{d_{tip}^2 \cdot \tan \alpha}$$

$$P_t = Y_s \cdot d_{tip}^2 \cdot \tan \alpha = 260 \text{ nN}$$

where  $d_{tip} = 100 \text{ nm}$  is the diameter of the needle tip, and  $\alpha = 15^\circ$  is the taper angle. The resulting failure load of 260 nN is two to three orders of magnitude larger than the force observed during cell penetration, and thus the needles as fabricated are not prone to yield failure. Another possible failure modality for the needle is buckling, for which it is also possible to evaluate the critical buckling load

$$P_{cr} = \frac{E}{240 \pi^2 L^2} [\pi^4 (b^4 + b^3 a + b^2 a^2 + b a^3 + a^4) + 20 \pi^2 (b - a)(a^3 + b^3) - 120(a + b)(b - a)^3] = 264 \text{ nN}$$

where

$E = 2.4 \cdot 10^9 \text{ Pa}$  is Young's modulus<sup>3</sup>  
 $a = 100 \cdot 10^{-9} \text{ m}$  is the tip diameter  
 $b = 600 \cdot 10^{-9} \text{ m}$  is the base diameter  
 $l = 5 \cdot 10^{-6} \text{ m}$  is the needle's length

The critical buckling load of 264 nN is also two to three orders of magnitude larger than the force experienced during cell penetration.

### Estimation of force necessary for penetration

The early literature about AFM-operated nanoneedles indicates that a force in the range of 0.5-2 nN per needles is necessary for intracellular penetration<sup>4</sup>. In our system the silicon chip employed measured 8x8x0.525 mm, weighing 70 mg. This chip, having a 2  $\mu\text{m}$  nanoneedles' pitch hosted  $1.6 \cdot 10^7$  needles. When accelerated at 100 rcf the chip would weigh 7g, equivalent to 68 mN, implying, for an equally distributed force, that each nanoneedle would experience 4.25 nN of force, above the threshold determined by AFM, but safely below the breakage forces estimated around 260 nN.

### Efficient loading and sustained release of nucleic acids.

Nanoneedles functionalized with aminopropyltriethoxysilane (APTES) efficiently loaded fluorescently-labeled siRNA. siRNA was found associated only on the external surface of solid silicon nanoneedles obtained through the same manufacturing process, yielding an extremely low, non-quantifiable loading efficacy (Figure S10). Porous nanoneedles significantly improved volumetric

loading of siRNA with uniform concentration across the whole nanoneedle's structure. The concentration of siRNA within the pores (0.1 nM) was three orders of magnitude higher than that of the loading solution. The loading of 10% of the siRNA in solution occupied only 1% of the available needle volume.

The porous structure of the needle also enabled the sustained release of siRNA. The drug release kinetics of siRNA exhibited a burst release of siRNA within the first 30 minutes, potentially attributable to siRNA loosely associated with the outer surfaces, followed by a sustained release over the next 18 hours (Figure S11) with 85% of the initial payload released within 12 hours. The prolonged release kinetics was analogous to the degradation profile of the needles, suggesting the role of nanoneedle architecture in the regulation of the drug release profiles.

## Supplementary Figures

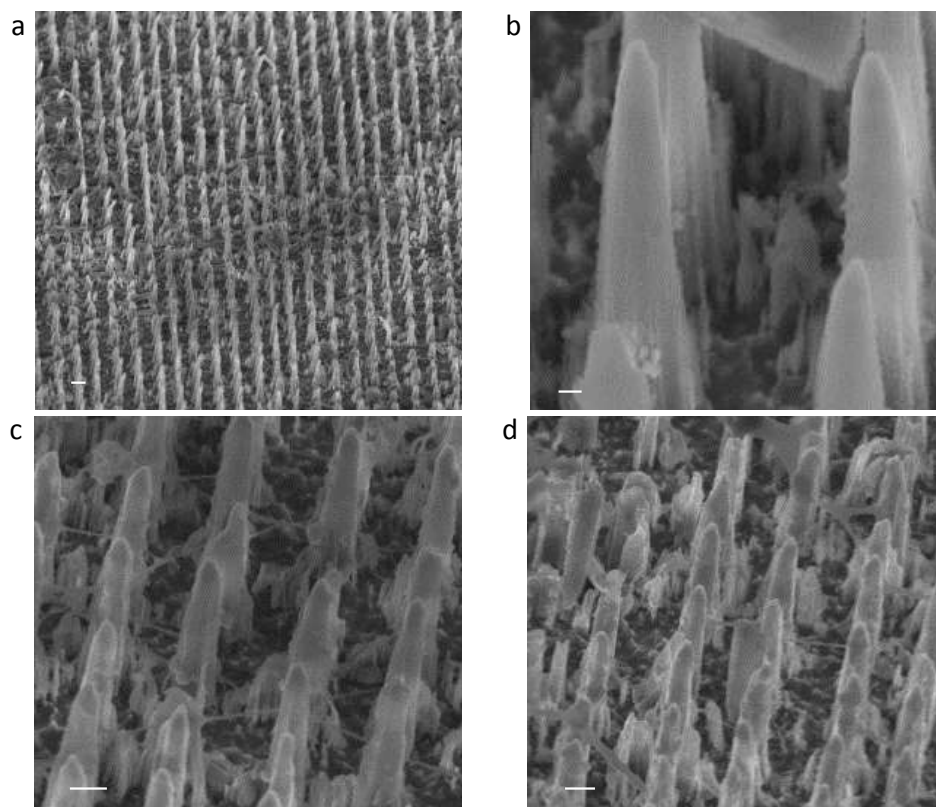


**Figure S1.** Nanoneedles integrity following imprinting. SEM imaging of nanoneedles chips pressed against animal tissue show their substantial integrity. The nanoneedles were pressed against: (a) skin on the back, (b) skin on the ear, (c-d) muscle. Scale bars: (a) 2  $\mu\text{m}$ , (b) 200 nm, (c-d) 1  $\mu\text{m}$ .



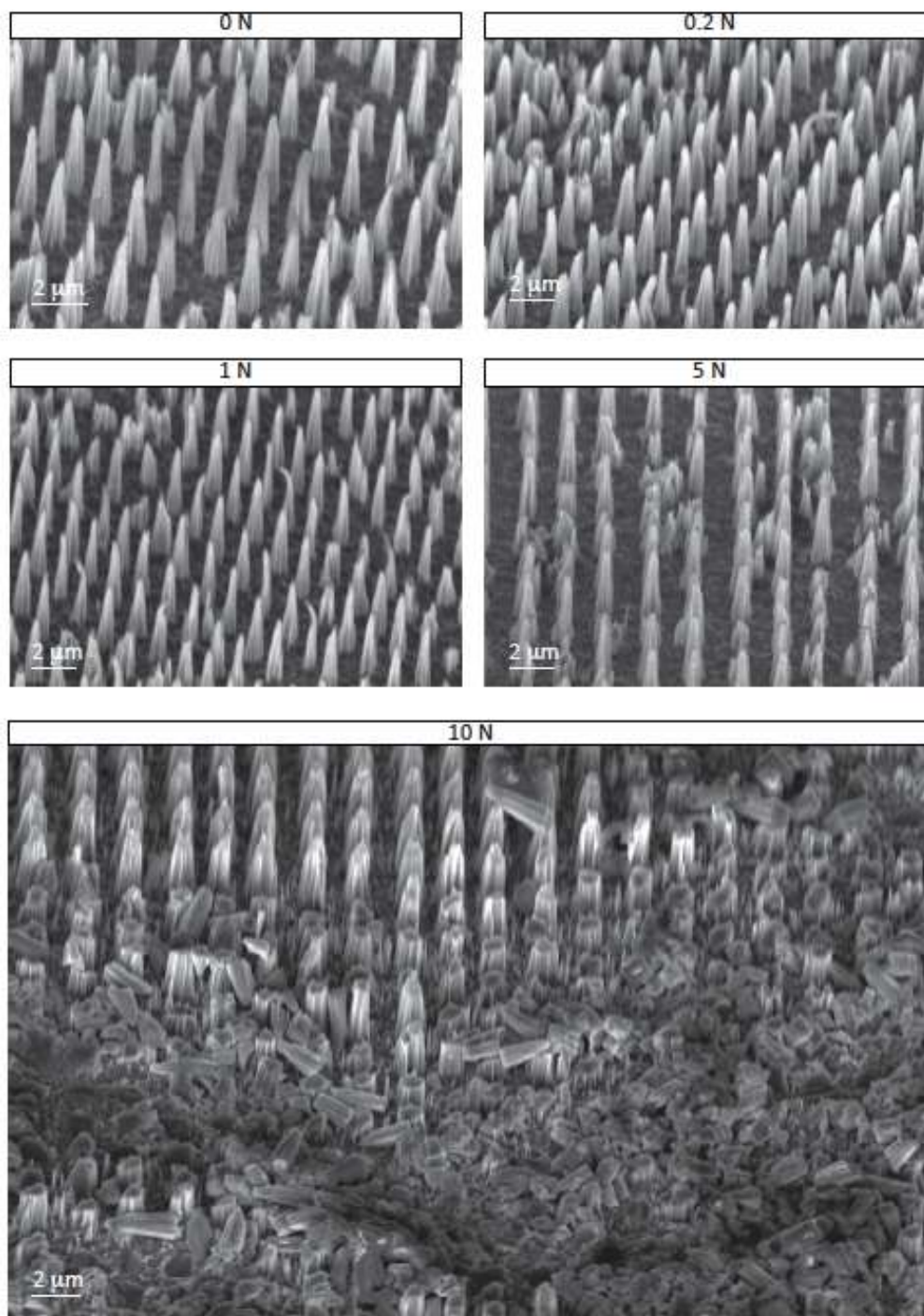


**Figure S2.** Compression testing of nanoneedles. SEM micrographs of nanoneedles subjected to increasing compressive forces. The peak force exerted on the nanoneedle chip is indicated at the top of each panel. Scale bars 2  $\mu\text{m}$ .

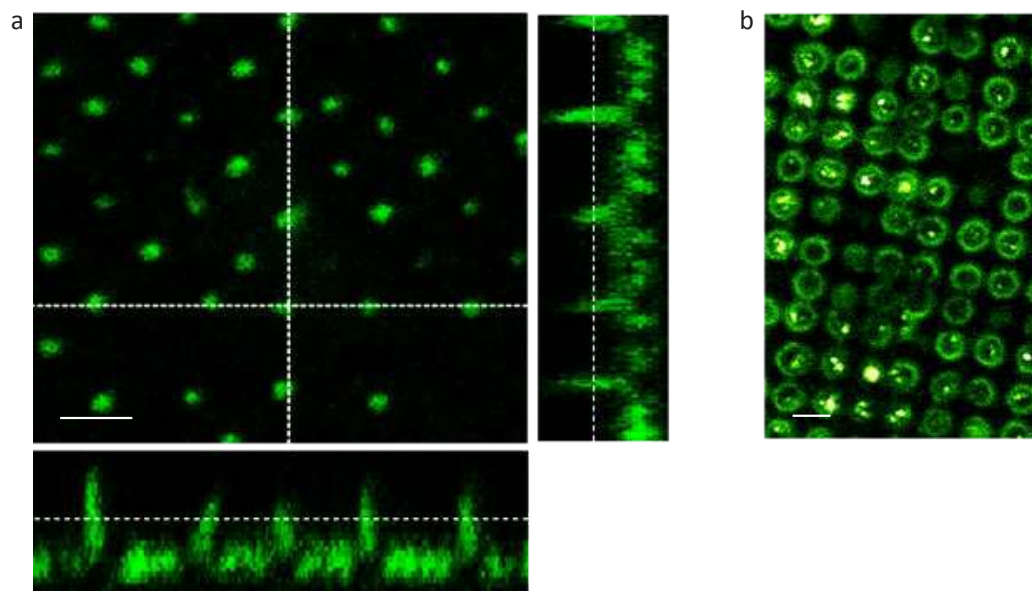


**Figure S3.** Volumetric Loading of siRNA. (a) Confocal microscopy z-stack of Cy3 fluorescent siRNA (green) loaded throughout the porous volume of pSi nanoneedles. (b) For comparison siRNA only loads over the surface of solidified nanoneedles. Scale bars 2 $\mu$ m.

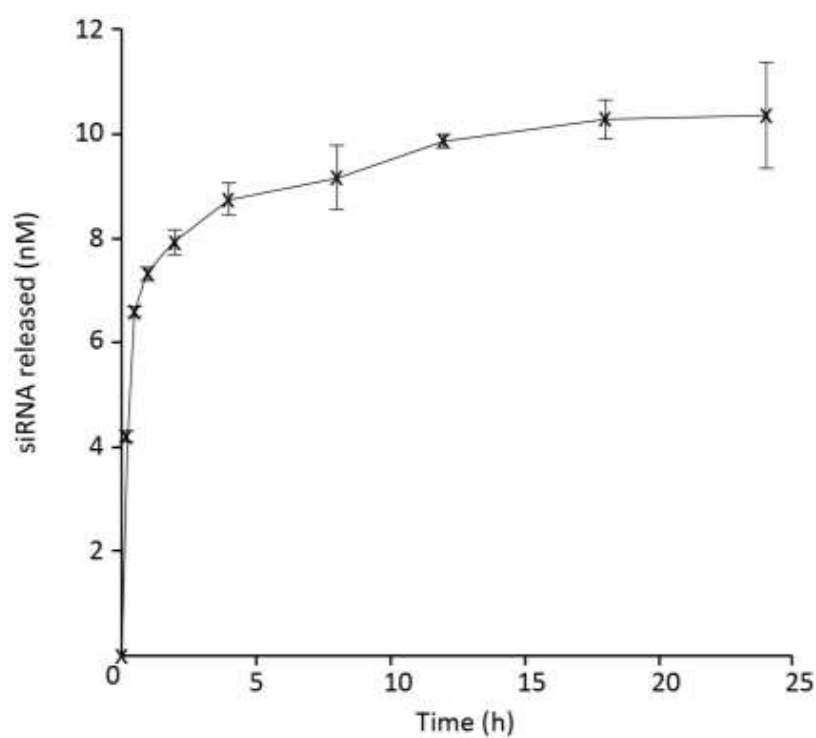


**Figure S4.** Sustained release of siRNA from pSi nanoneedles in PBS. Quantification of siRNA release kinetics from nanoneedles over 24 hours.

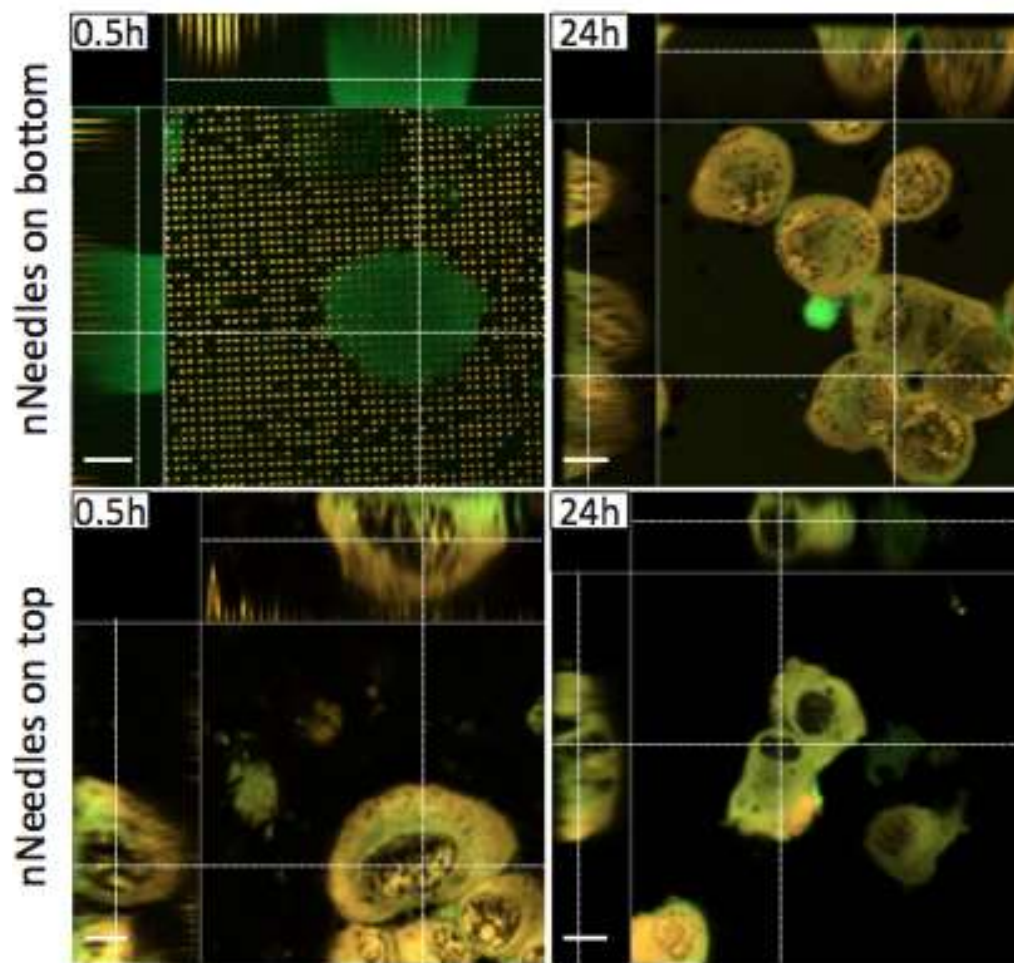


**Figure S5.** siRNA delivery through nanoneedles. Confocal microscopy z-stacks of nanoneedles interfaced with cells, showing cytosolic localization of siRNA. nN-B show siRNA delivery at 24 hours following interfacing, while nN-T show siRNA delivery at 30 minutes following interfacing. Cells stained with Celltracker Green (green) and fluorescent Cy-3-siRNA (yellow). Scale bars 10  $\mu$ m.



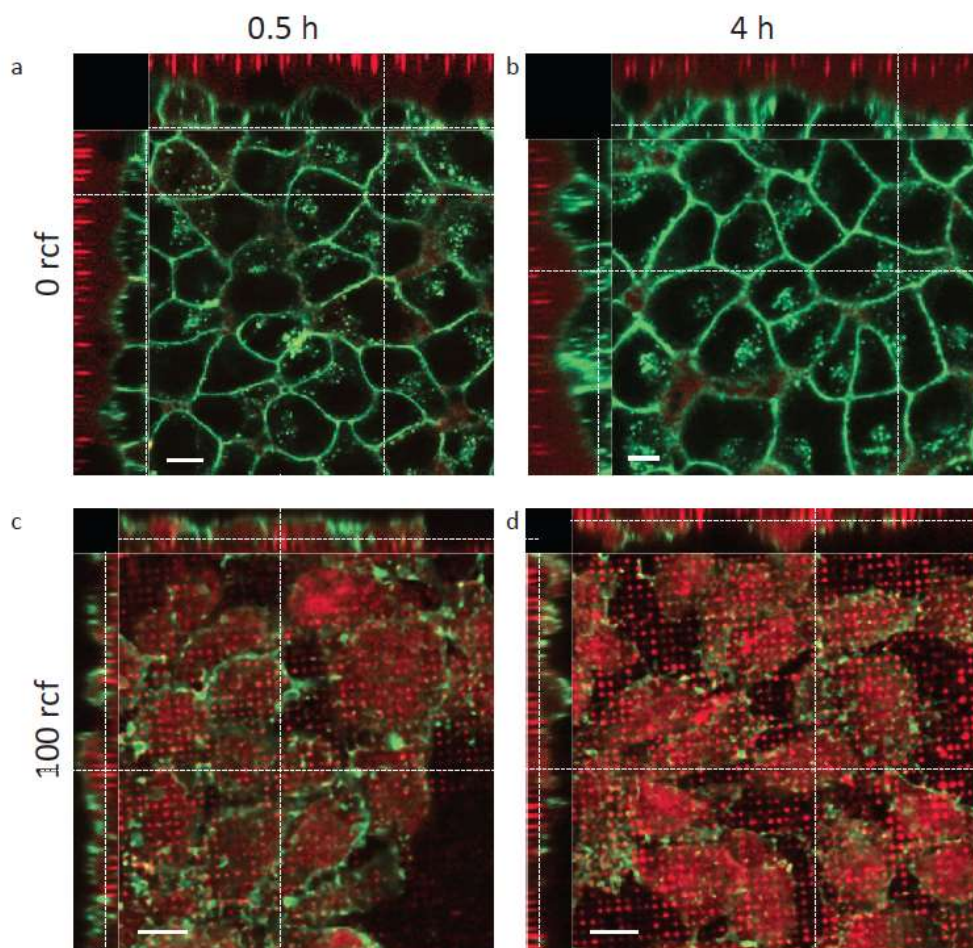


**Figure S6.** nN-T interfacing without application of force does not induce intracellular delivery of Cy3-siRNA. Confocal micrographs comparing nN-T interfacing without application of force (a, b) and with application of 100rcf force by centrifugation (c, d) at 30 minutes (a, c) and 4 hours (b, d) following initial interfacing. During the entire duration of the experiment the cells were maintained at 4 °C to prevent active internalization. Cy3-siRNA in red, and cell membrane in green. Scale bars 10 μm

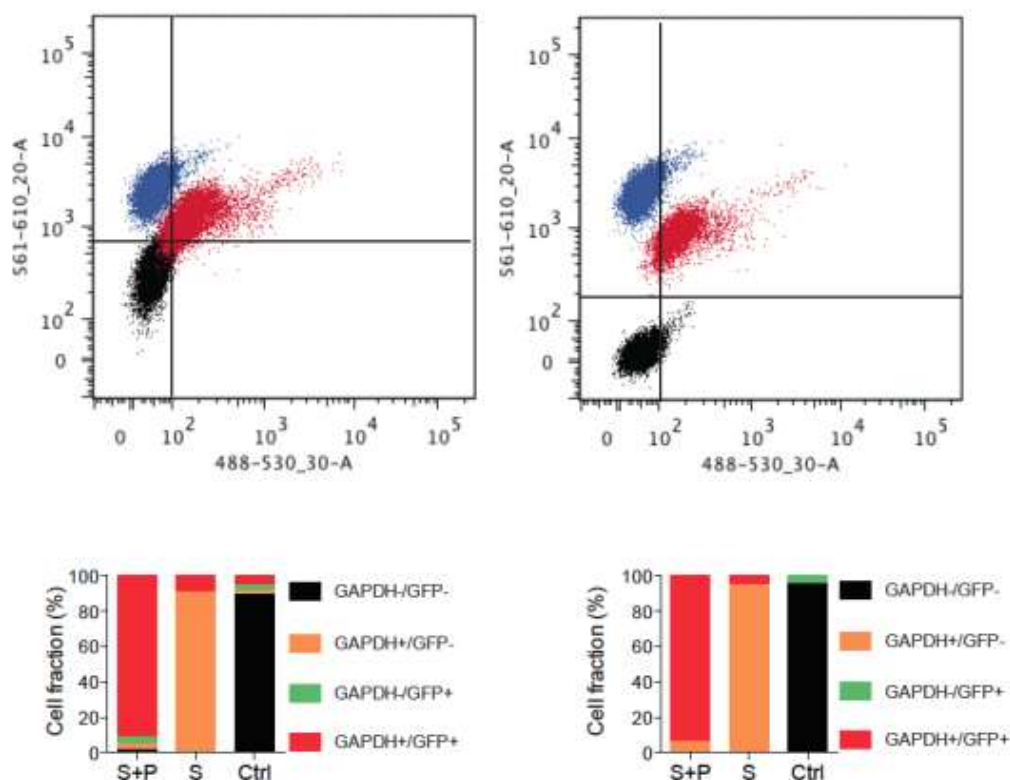


**Figure S7.** Flow cytometry biological replicate indicating successful GFP and GAPDH siRNA expression. The two scatter plots show the fluorescence intensity in the GFP (x-axis) and Cy3 (y-axis) channels for two biologically independent flow cytometry experiments comparing cells transfected with Cy3-GAPDH-siRNA (blue), Cy3-GAPDH-siRNA and GFP plasmid (red), and empty nanoneedles (black). The two graphs quantify the flow cytometry data according to the quadrant gates displayed.

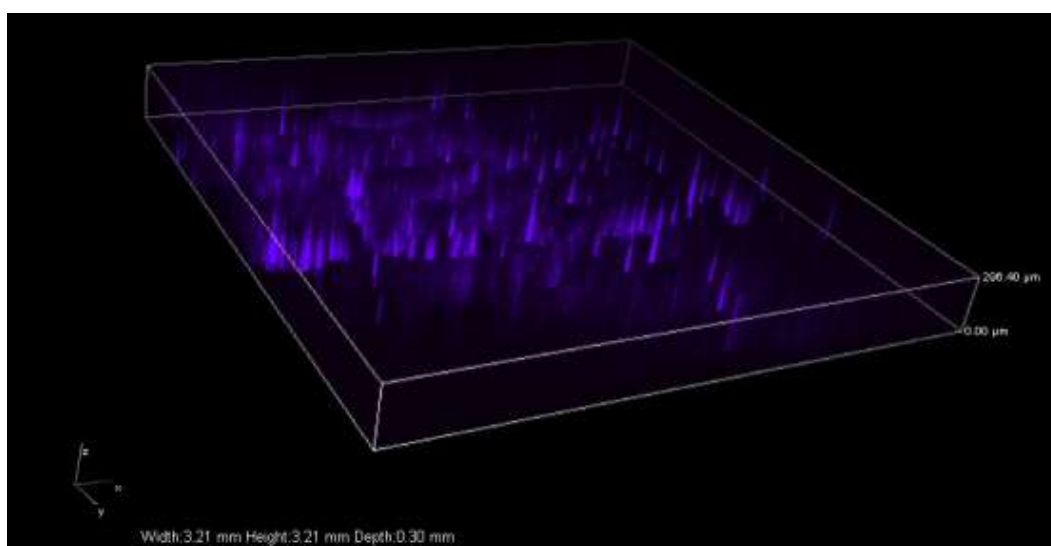


**Figure S8.** Three dimensional intravital confocal microscopy of dye-conjugated nucleic acids localized to the surface of the target tissue acquired 1 hour following imprinting.

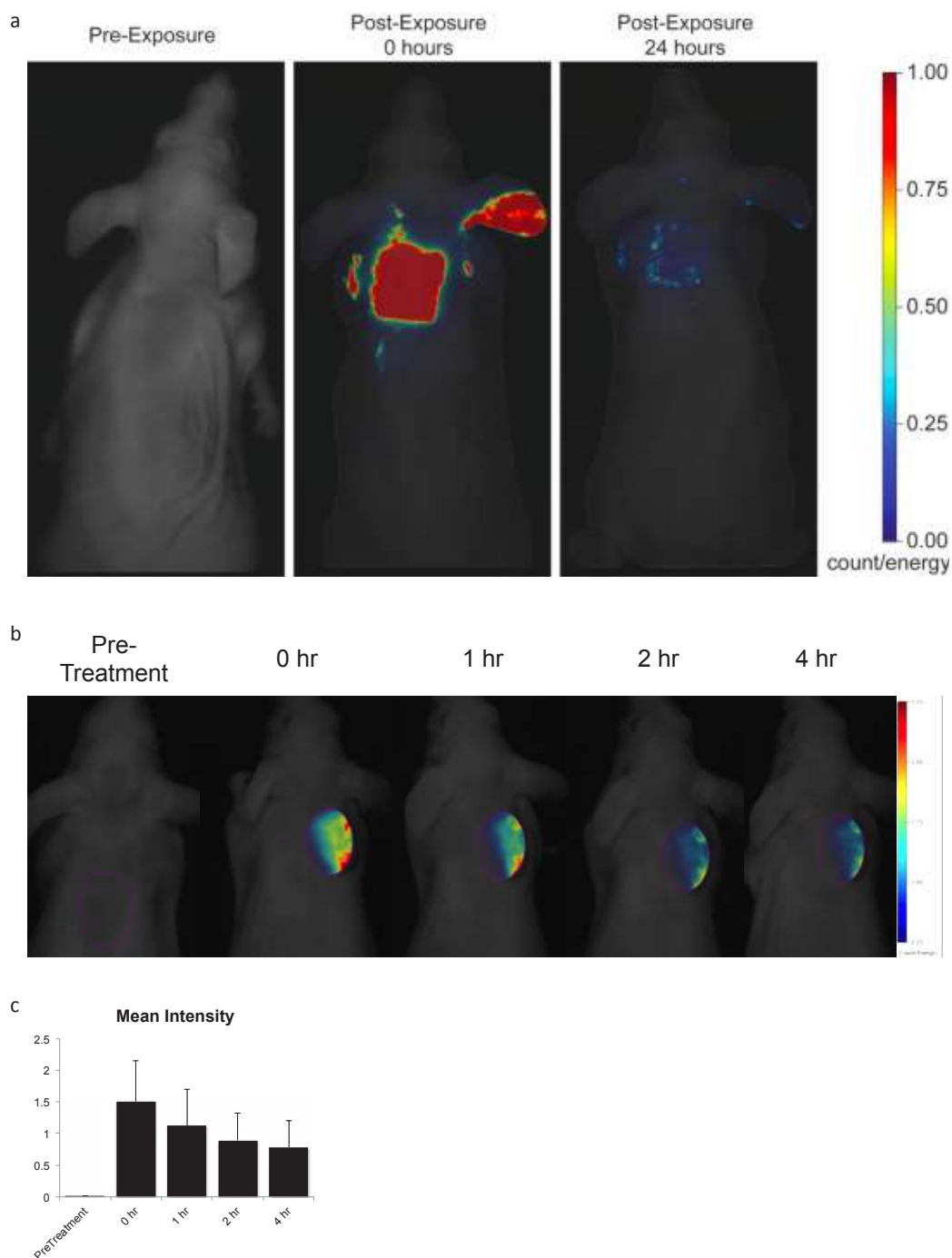


**Figure S9.** *In vivo* comparison between delivery sites. Near infrared fluorescent imaging on the skin of mice comparing the delivery of VivoTag-S 750 imaged using the VisEn FMT 2000 system (Perkin Elmer) to the skin of the back and to the ear (a) and to the muscle (b). Delivery to the skin of the ear followed the same trend as delivery to the skin of the back, and delivery to the muscle also showed localization and prolonged retention (c), similar to that observed for delivery to the skin.



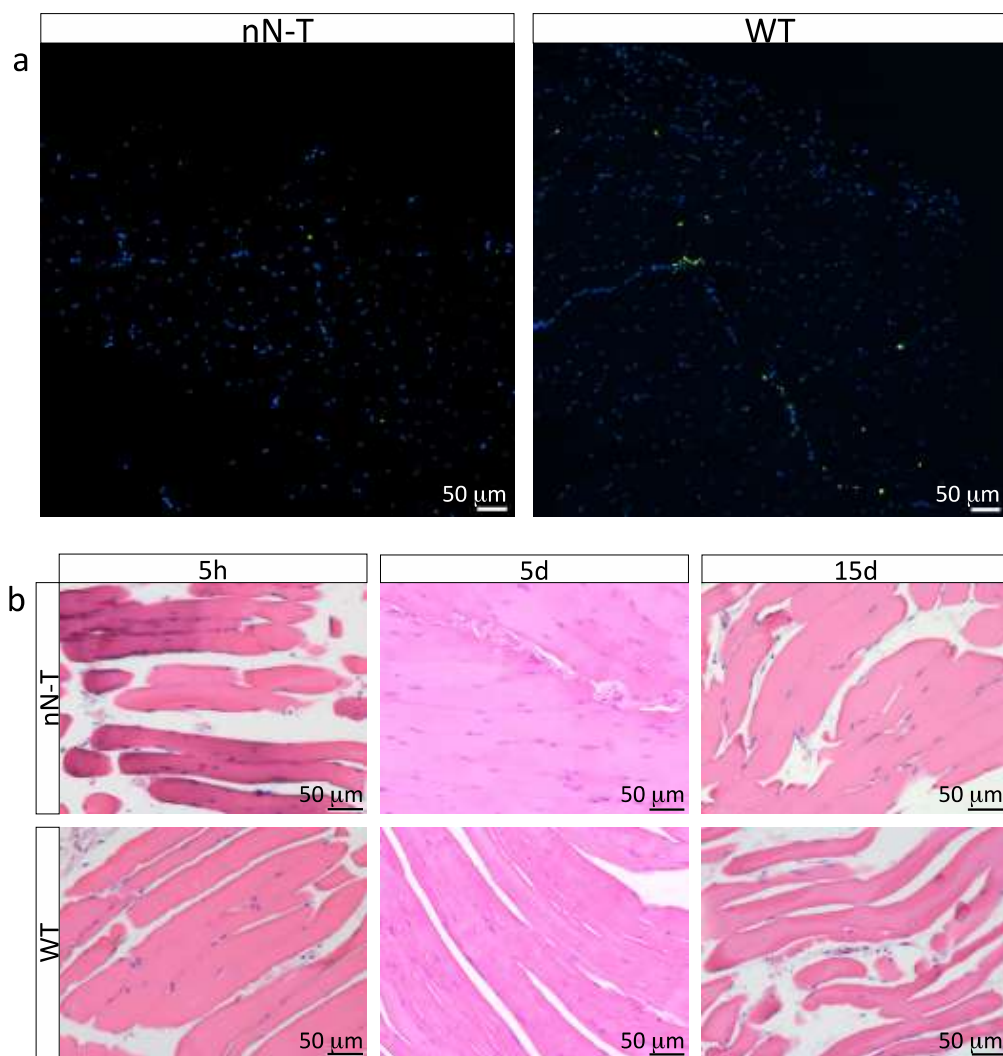


**Figure S10.** Nanoinjection has minimal impact on macrophage infiltration and muscle structure. (a) nN-T nanoinjected muscle exhibit minimal positive staining for macrophages (green), similar to what observed for WT (normal) muscle sections. Nuclei in blue. (b) Longitudinal muscles sections: nN-T nanoinjection is compared to control sections at 5 hours, 5 days, and 15 days showing negligible effect on these sections similar to what was observed in Figure 4 with transverse sections.

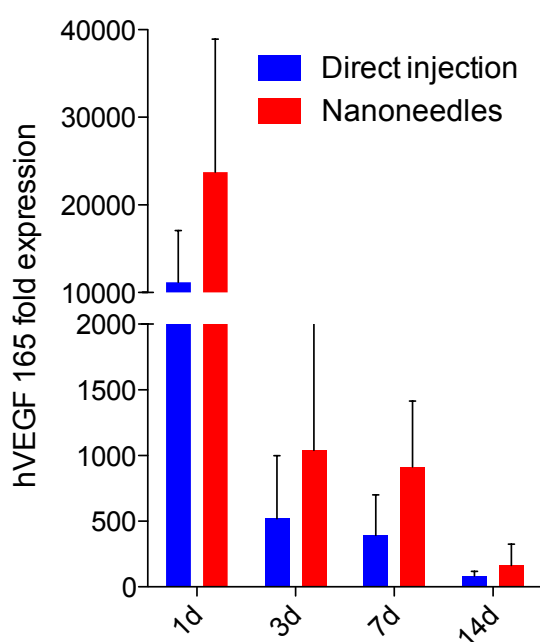


**Figure S11.** Real time PCR quantification of hVEGF 165 expression delivered either by direct intramuscular injection or nanoinjection. Single treatment performed at day 0.

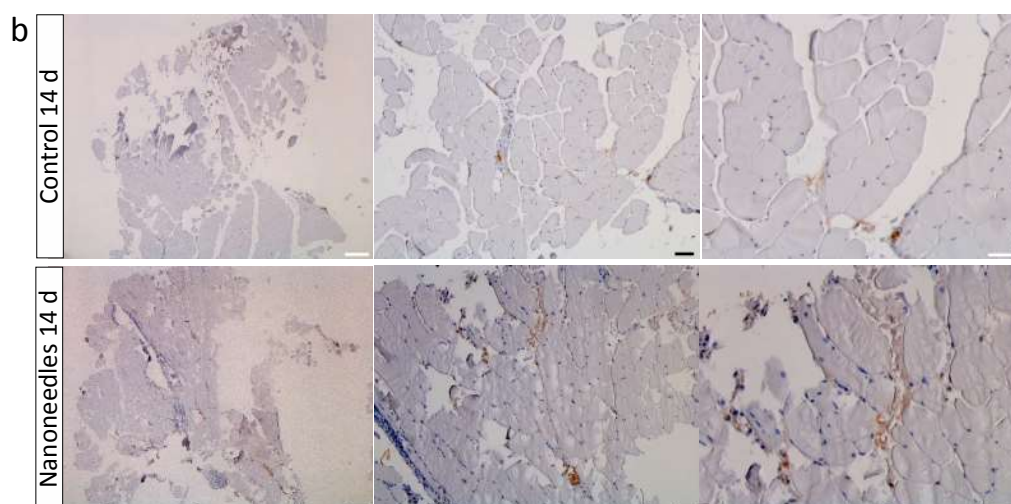


**Figure S12.** Immunohistochemical analysis of neovasculture formation within the tissue following treatment with nanoneedles. Staining with CD31 for untreated (top) and nanoneedles treated (bottom) muscle. Scale bars from left to right 200  $\mu\text{m}$ , 50  $\mu\text{m}$ , 50  $\mu\text{m}$ .

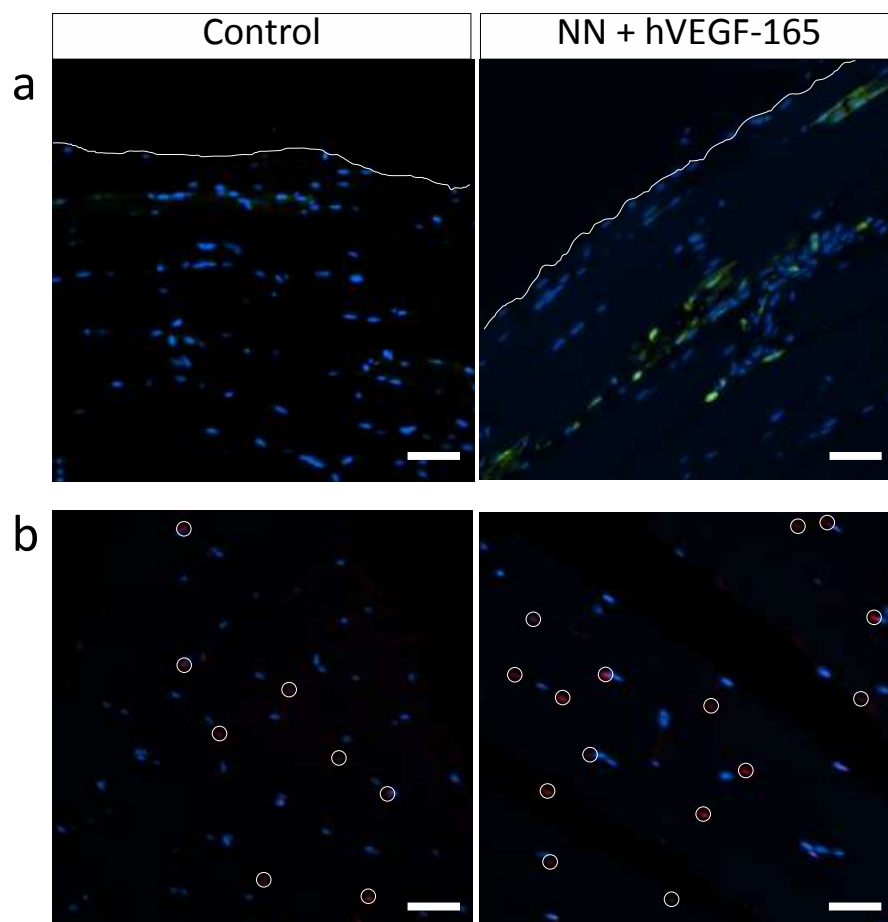


**Figure S13.** Vessel profile following nanoinjection. (a) Transverse muscle sections showing arterioles (green) in proximity of the injection surface (white) of nanoinjection as compared to control. (b) Muscle sections showing capillaries (red signal, circled in white) density in proximity of the injection area. Scale bars: (a) 50  $\mu\text{m}$ , (b) 25  $\mu\text{m}$ .

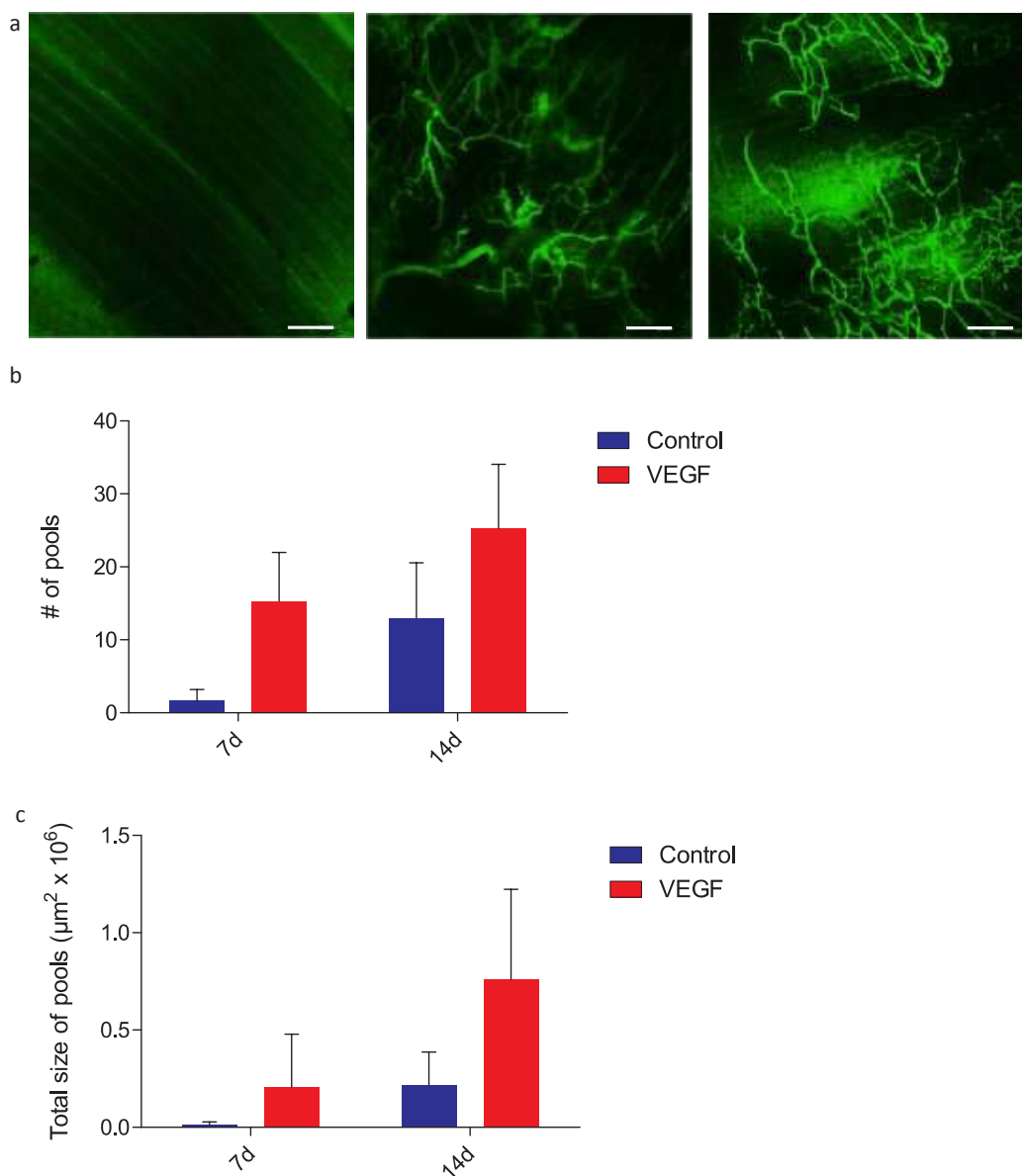


**Figure S14.** Intravital microscopy quantification of vessels extravasation. (a) Intravital microscopy confocal images for muscle untreated (left) and nanoneedles treated after 7 (center) and 14 days (right) with (b,c) relative image analysis showing (b) number and (c) size of extravasations pools at 7 and 14 days. Scale bars 50  $\mu\text{m}$ .

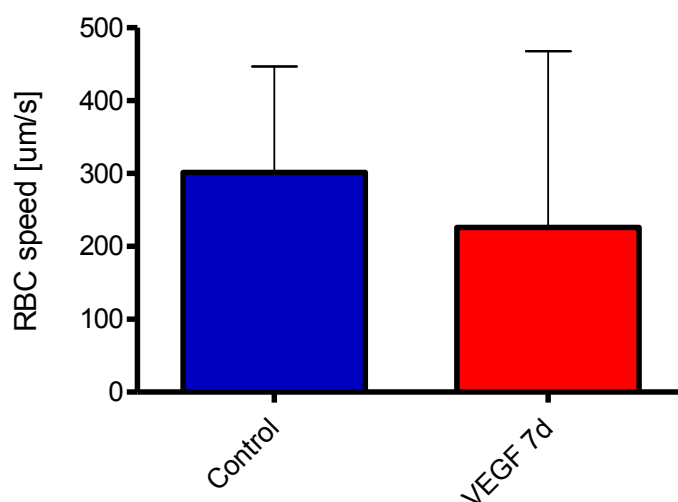


**Figure S15.** Comparison of red blood cell flow rates vessels following treatment. Speed measurement of red blood cells (RBC) flowing in the muscle vessels before and after the nanoneedles treatment with pVEGF. Similar flow rates were observed in the treated and untreated tissue thus confirming that newly formed vessels retained physiological circulatory functions.

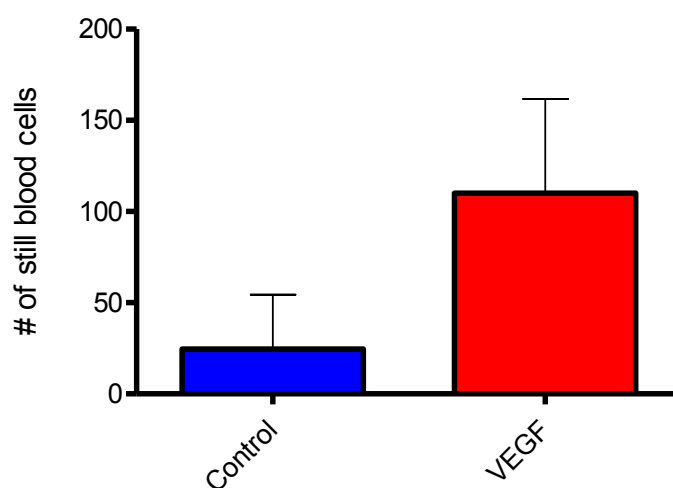


**Figure S16.** Quantification of stationary RBC in muscles. The number of blood cells that exhibited minimal movement or stationary in the muscle vessels before and after the nanoneedles treatment with pVEGF was evaluated. The significant (four-fold) increase of stationary RBC in the treated tissue suggests an undergoing process of muscle regeneration.

## Supplementary Movie Captions

**Movie S1.** Live imaging of blood flow in control tissue. Montage of DiD-stained red blood cells flowing within muscle vessels after IV injection of FITC-conjugated dextran. RBC flows freely in the newly formed vessels within the muscle following a straight and parallel pattern.

**Movie S2.** Live imaging of blood flow in nanoneedles treated tissue. Montage of DiD-stained red blood cells flowing within muscle vessels in area treated with pVEGF-loaded nanoneedles after IV injection of FITC-conjugated dextran. The majority of RBC flow within the vessels of the muscle follows their typical random pattern while several appear stationary. This observation may reveal the presence of several macrophages and was quantified in Figure S14.

**Movie S3.** Live imaging of vessels in the muscle treated with pVEGF-loaded nanoneedle directly after IV administration with FITC-conjugated dextran. The increase in fluorescence along the vessels of the nano-injected tissue following the administration of a labeled tracer demonstrated the preserved functional features of all the newly formed vessels. This data was also confirmed by the flow rate quantification performed in Figure S13.



## Materials and Methods

### Patterning of Si wafers

Si wafers (100 mm, 0.01  $\Omega$ -cm, boron doped p-type, Silicon Quest International, USA) were cleaned by piranha treatment ( $\text{H}_2\text{O}_2$ : $\text{H}_2\text{SO}_4$  1:2 8 min). A masking layer of 160 nm low stress silicon nitride was deposited by low pressure chemical vapor deposition (835  $^\circ\text{C}$ , 300 mTorr,  $\text{SiH}_2\text{Cl}_2$ / $\text{NH}_3$  80:20%, 40 min) over the Si wafers. A 250 nm thick layer of Futurrex NR9-250P photoresist (Futurrex Inc., USA) was spun over the substrate (40 s, 4000 RPM, 5000 RPMS), and pre-baked for 3 minutes at 70  $^\circ\text{C}$ . The photolithographic pattern consisting of 600nm diameter disks with a pitch ranging from 2  $\mu\text{m}$  to 20  $\mu\text{m}$  (Photronics, USA) was transferred on the substrate in a K. Suss MA-6 mask aligner (K. Suss, Germany) with a 70 mJ/cm<sup>2</sup> dose. The substrate was hard baked for 1 min at 100  $^\circ\text{C}$  and then developed for 12 s in a 1:3 v:v mixture of RD6 developer (Futurrex Inc, USA) and deionized water. The pattern was transferred into the silicon nitride layer by reactive ion etch with  $\text{CF}_4$  plasma for 120 s, insuring that no etch-through to the silicon would occur (Plasmatherm 790 series, 15 sccm  $\text{CF}_4$ , 200 mTorr, 250 W RF power). The photoresist was stripped by piranha clean for 8 minutes, followed by the removal of the silicon nitride residual scum layer in 49% HF for 5 minutes. The substrate was stored in a cleanroom environment until further use.

### Synthesis of nanoneedles by metal assisted chemical etch

The patterned Si wafer was cleaned in 10% HF for 60 s followed by deposition of Ag in a solution with 5ml  $\text{AgNO}_3$  (0.02M, Sigma Aldrich), 20ml 49% HF, 75ml  $\text{H}_2\text{O}$  forming Ag nanoparticles and dendrites selectively over the exposed Si area (not over the silicon nitride mask for 2 m). The substrate was rinsed in water and 2-propanol, and dried. Metal assisted chemical etch of the substrate in 80 ml HF, 316 ml  $\text{H}_2\text{O}$  and 5 ml  $\text{H}_2\text{O}_2$ , for 8 min 30 s formed porous silicon pillars with 600 nm diameter and 9  $\mu\text{m}$  height underneath the silicon nitride pattern interspersed with porous silicon nanowires in the field. The pillars were shaped into cones with apical diameter < 50 nm by reactive ion etch in  $\text{SF}_6$  plasma (Oxford 80 series, 20 sccm  $\text{SF}_6$ , 100 mTorr, 250 W RF power, 2 min 30 s). The  $\text{SF}_6$  plasma etching also removed the silicon nitride mask and the nanowire grass in the field. The 100 mm Si substrate was cut in 8 x 8 mm chips with a dicing saw, and the nanoneedles on the chips were oxidized by  $\text{O}_2$  plasma for 10 minutes ( $\text{O}_2$  20 sccm, 150 W, 0.4 mBar). The resulting substrates were stored until needed.

### Controlling Nanoneedles' Porosity

The porosity of the nanoneedles was controlled by tuning the parameters of the metal assisted chemical etch according to published protocols<sup>5</sup>.

### Controlling Nanoneedles' Diameter

The diameter of the nanoneedles was controlled by tuning the duration of the  $\text{SF}_6$  plasma etch. A 1 m 30 s etch returned nanoneedles with 400 nm diameter, which required removal of the nitride caps by wet etch in 49% HF, and a 2 m etch returned nanoneedles with 200 nm diameter.

**Mechanical testing of Nanoneedles**

Mechanical compression of the nanoneedle arrays was performed with a Bose Electroforce® 3200 Series II test instrument (Bose Ltd, UK) equipped with a 5 lbf (22N) load cell. Compression was performed on at a constant rate of 10 nm/sec, to a peak load of 10N and 100 nm/sec to a peak load of 5N, 1N, or 0.2N. Load was applied to the entire surface of the array, corresponding to  $1.6 \times 10^7$  nanoneedles.

**Cell Culture**

HeLa cells were used throughout the study, cultured in Dulbecco Modified Essential Medium, supplemented with 10% v:v fetal calf serum and 1% v:v antibiotic/antimycotic. Cells were maintained in a 5% CO<sub>2</sub> incubator at 37 °C throughout the culturing period. Human dermal fibroblasts (HDF) were a gift from the lab of Dr. Rita Serda (HMRI) and were originally purchased from ATCC. HDF were maintained using fibroblast basal media supplemented with fibroblast growth kit – low serum (ATCC).

**Nanoinjection: Nanoneedles on bottom**

An 8 x 8mm nanoneedle chip was sterilized in 70% ethanol for 1 h and allowed to dry under UV irradiation. The chip was placed at the bottom of a 24 well plate and rinsed thrice with PBS. The desired density of cells (typically around  $1 \times 10^5$  cells) was seeded over the needles and the well plate was returned to the incubator.

**Nanoinjection: Nanoneedles on top**

Cells were seeded at  $5 \times 10^4$  cells on the bottom of a 24 well plate and incubated for 24-48 hours until reaching >60% confluence. The cell culture medium was exchanged with 3 ml of fresh medium and the nanoneedle chip was immersed in medium face down. The plate was transferred to a swinging bucket centrifuge with appropriate counterweight and spun at 100 rcf for 1 m. If further culturing was required, the chip was then removed from the well after 30 minutes of incubation and placed face up in a different 24 well plate, covered with 0.5 ml of medium. Otherwise the chip was removed and fixed.

**MTT Assay**

nN-B: For each time point  $2 \times 10^4$  cells were seeded with the nanoneedles on bottom configuration in triplicate at day 0 in a 24 well plate (Corning). At each timepoint MTT reagent (thiazolyl blue tetrazolium bromide, Sigma Aldrich) was added to each well to a final concentration of 0.5 mg/mL and incubated for 2 h at 37 °C. The medium was then aspirated and the reduced product solubilized in 400 µl/well of dimethyl sulfoxide (DMSO). Absorbances were measured at 570 nm in a microplate reader (Biotech Synergy H4). Cells grown on 8 x 8mm flat silicon substrates were employed as a negative control.

nN-T: For each time point  $2 \times 10^4$  cells were seeded triplicate nN-T at day 0 in a 24 well plate (Corning). At each timepoint MTT reagent (thiazolyl blue tetrazolium bromide, Sigma Aldrich) was added to each well to a final concentration of 0.5 mg/mL and incubated for 2 h at 37°C. The medium was then aspirated and the reduced product solubilized in 400 µl/well of dimethyl sulfoxide (DMSO). Absorbances were measured at 570 nm in a microplate

reader. Cells grown on 8 x 8mm flat silicon substrates were employed as a negative control.

### **LDH Assay**

A lactate dehydrogenase (LDH) assay (Abcam) was used to study the release of LDH from HDF upon exposure to pSi nanoneedles.  $3.5 \times 10^4$  HDF were seeded into 24 well plates and treated with 0.25% v:v Triton X-100, nN-T, nN-B, regular silicon wafers (Ted Pella), or sterile phosphate buffered saline (PBS). Each sample was carried out in quadruplet and at pre-determined times 25  $\mu$ L of media was removed and centrifuged at 600 rcf for 5 minutes. A 10  $\mu$ L aliquot was removed and mixed with 100  $\mu$ L of LDH assay buffer mix in a 96 well plate. Samples were incubated for 30 minutes at room temperature and were measured on a Synergy H4 (BioTek) plate reader at OD of 450 nm.

### **SEM analysis of nanoneedles interfacing**

Cells were interfaced either nN-B or nN-T, and then fixed at the desired timepoint with 0.2% v:v glutaraldehyde in phosphate buffered saline for 15 minutes. The substrates were then dehydrated over a graded ethanol series (10%, 30%, 50%, 70%, 90%, 2x 100%) for 5 minutes at each passage. Finally the substrates were treated with hexamethyldisilazane (HMDS, Sigma Aldrich) for 5 minutes and allowed to dry. The samples were sputter coated with 10 nm of Cr and imaged by in-lens detector in a Carl Zeiss Neon 40 SEM with acceleration voltages ranging from 1.4 keV to 5 keV.

### **SEM/FIB cross sectional analysis of nanoneedles interfacing**

Cells were interfaced either nN-B or nN-T, and then fixed at the desired timepoint with 0.2% v:v glutaraldehyde in phosphate buffered saline for 15 minutes. The substrates were then dehydrated over a graded ethanol series (10%, 30%, 50%, 70%, 90%, 2x 100%) for 5 minutes at each passage. The substrates were stained with 2% osmium tetroxide/ 2% potassium ferrocyanide in cacodylate buffer, then embedded with increasing Epon 812 substitute concentration in ethanol (v/v): 2:1 for 2 hours, 1:2 for 2 hours, 1:2 overnight (Electron Microscopy Sciences, USA). Excess resin on the surface was gently but thoroughly washed with ethanol from a wash bottle so that the remaining resin was conformal to the needles and cells on the substrate. The resin was cured for 48 hours at 60 °C. The samples were sputter coated with 10 nm of Cr and analysed in a Carl Zeiss Auriga SEM/FIB equipped with a Ga ion beam and in-lens backscattering detector. Coarse milling was performed with a 120 pA aperture and fine milling was performed with a 50 pA aperture. Images were acquired at 54° tilt through the in-lens backscattering detector at the eucentric working distance and with an acceleration voltage of 1.4 keV.

### **Confocal Microscopy of nanoneedles interfacing**

Cells were interfaced either nN-B or nN-T, and then fixed at the desired timepoint with 4% paraformaldehyde in phosphate buffered saline for 15 minutes. The cell membranes and nuclei were stained respectively with AF594-wheat germ agglutinin (5  $\mu$ g/mL, 10 min) and DAPI (300 nM, 3 m). The nanoneedle substrate had been previously stained with FITC. First a layer of 3-aminopropyltriethoxysilane (APTES, Sigma Aldrich) was formed on the oxidized nanoneedles by liquid phase conjugation in a 2% v:v ethanoic solution of APTES

for 2 h. The APTES layer was stabilized by baking at 120 °C for 1 h. FITC was conjugated to the free amine on the APTES molecules from a 0.01 mg/ml solution in phosphate buffered saline for 1h. The needles were washed repeatedly and used for interfacing. The samples were mounted on a coverslip with Prolong Gold antifade Reagent (Life Technologies, USA) and analyzed on a Leica SP5 inverted confocal microscope (Leica, Germany) or a Nikon A1 inverted confocal microscope (Nikon, USA).

### ICP-AES

Inductively coupled plasma – atomic emission spectroscopy (ICP-AES Varian 720-ES) was used to investigate the degradation of pSi nanoneedles in a physiological simulated environment. pSi nanoneedles were individually placed in a 24 well plate and submersed in 1.5 mL of sterile PBS, placed on a rocking platform, and incubated in an oven set at 37 °C for 140 hours. At pre-determined times samples were removed for ICP-AES and SEM. For ICP samples, 1 mL of PBS was removed, stored at 4 °C until further analysis, and pSi nanoneedles were replenished with 1 mL of new PBS. Samples for ICP-AES were diluted 1 to 50 in water and measured for silicon content at the following wavelengths: 251.432, 250.690, 251.611 and 288.158 nm.

### siRNA loading

The chips surface was functionalized with 3-aminopropyltriethoxysilane (APTES) as described in the “Confocal Microscopy of nanoneedles interfacing” section of the methods. GAPDH cy3-siRNA was loaded within the APTES functionalized porous structure. 50 µl of 100 nM Cy3-siRNA in PBS was spotted on the nanoneedles chip and incubated for 15 minutes. Following incubation the chips were rinsed three times with 100 µl of DI water. Loading within the porous structure was assessed by confocal microscopy. The loading concentration was assessed by full dissolution of the nanoneedles in 1M KOH, followed by quantification through UV-Vis absorption at 260 nm (Nanodrop, Thermo Scientific Inc, USA). Experiments were run in triplicate.

### siRNA release

APTES functionalized chips loaded as previously described with Cy3-siRNA were employed for a passive payload release study. The chips were incubated for 24 h in 100 µl of PBS at room temperature. At fixed timepoints (10 m, 30 m, 1 h, 2 h, 4 h, 8 h, 12 h, 18 h and 24 h) 10µl of solution was aliquoted for analysis at spectrofluorometer. 10 µl of PBS was added at each timepoint to preserve solution volume. The change in concentration resulting from addition of solution was taken into account in the reported results. Cy3 fluorescence was quantified in a 10 µl volume quartz cuvette in a Jobin Ivon spectrofluorimeter (HORIBA, UK). Experiments were run in triplicate.

### siRNA delivery *in vitro*

GAPDH-Cy3-siRNA was loaded on the nanoneedles as previously described. Nanoneedles were interfaced either nN-T or nN-B with cells. At 30 minutes and 24 hours following treatment the cells were fixed in 4% v:v paraformaldehyde in phosphate buffered saline for 15 minutes, mounted on a coverslip with Prolong Gold antifade Reagent (Life Technologies, USA) and analysed on a Leica SP5 inverted confocal microscope (Leica, Germany).

**In-cell western for GAPDH silencing**

siRNA was loaded onto the nanoneedles as described above in the confocal microscopy of nanoneedles interfacing method. The nanoneedles were interfaced nN-B and cells were cultured for 24 hours. For the siRNA delivered from solution control, the same amount of siRNA loaded onto the needles was added in solution 4 hours following cell seeding, in order to prevent siRNA adsorption to the needles and its subsequent delivery from therein. Samples were washed thrice in phosphate buffered saline and fixed in 4% v:v paraformaldehyde. The cells were permeabilised for 20 minutes in 0.25% v:v Triton-X in phosphate buffered saline (PBS) and blocked with Superblock in PBS (Thermo Scientific, USA) for 30 m. The cells were incubated with monoclonal anti-human GAPDH antibody raised in mouse (AbCam, USA) mixed with DRAQ 5 staining for DNA quantitation (0.5 nM) in Superblock PBS for 1 h at room temperature. The samples were washed 5 times in Superblock PBS for 5 m each and then incubated with anti-mouse IGG antibody conjugated to IR DYE-800cw (Licor, USA). The samples were washed thrice in Superblock PBS and analysed in a Licor Odyssey infrared scanner (Licor, USA). GAPDH expression was quantified from the fluorescent intensity at 800 nm normalized to the total chip surface area. GAPDH expression for cells grown on empty nanoneedles and nanoneedles loaded with scrambled siRNA were used as the negative controls.

**siRNA and GFP plasmid loading, delivery and expression *in vitro***

APTES functionalized chips were incubated with 20  $\mu$ l of GAPDH cy3-siRNA (100 nM) and GFP plasmid (500 ng/ $\mu$ l, pRRLSIN.cPPT.PGK-GFP.WPRE deposited with addgene, courtesy of Dr. Manuel Mazo) for mammalian expression in PBS. The solution was allowed to dry over the nanoneedles, and the needles were immediately employed in a nN-B strategy. For confocal microscopy analysis the cells were fixed in 4% v:v paraformaldehyde for 15 minues at 48 hours following transfection. For flow cytometry analysis the cells were trypsinized, collected in a 1 ml microcentrifuge tube, centrifuged at 300 rpm, washed twice with phosphate buffered saline and then fixed in 0.5% v:v paraformadelhyde for 1 h. The samples were immediately analyzed on a Fortessa Flow Cytometer (GE Healthcare, USA) and the data was processed with FlowJo (TreeStar Inc, USA). Cells cultured on nanoneedles without nucleic acid loading were used as a negative control.

**Nanoneedles treatment *in vivo***

Animal studies were performed in accordance with the guidelines of the Animal Welfare Act and the Guide for the Care and Use of Laboratory Animals based on approved protocols by The University of Texas M.D. Anderson Cancer Center's (MDACC) and Houston Methodist Research Institute's (HMRI) Institutional Animal Care and Use Committees. Prior to administration to mice, chips were thoroughly cleaned and dried under UV and sterile conditions to ensure the removal of impurities on the pSi nanoneedles surface and then incubated with 20  $\mu$ L of fluorescent dyes (1 mg/mL) or plasmid VEGF (vascular endothelial growth factor)-165 at a concentration of 5 mg/mL in PBS. The solution was allowed to dry over the nanoneedles, and the needles were immediately employed.



For fluorescent dye experiments, imaging was performed at MDACC. Female athymic nude mice (NCR-Fox1<sup>nu</sup>; 4-6 week old) were purchased from Charles Rivers Laboratories and maintained as previously described<sup>5</sup>. For studies where pSi nanoneedles were placed under the skin, a small incision was made on the upper-back right of the mouse and sutured using staples. Nanoneedles were pressed down using the thumb ensuring minimal movement of needles for at least 1 minute. Then needles were removed and the incision was sutured if necessary.

Plasmid VEGF delivery was performed at HMRI. Male nude mice were anesthetized and a 1-2 cm dorsal midline incision was made to expose the superficial gluteal and lumbar muscles. The fascia was gently elevated from the underlying muscle and VEGF loaded pSi nanoneedles were implanted in direct contact with the lumbar and gluteal muscle on the right side, while the left side was left untreated. Nanoneedles were pressed down left in contact with the muscle for a minute using the user's thumb while ensuring the needles themselves experienced minimal movement. Needles were then removed, the fascia was replaced, and the skin was closed using wound clips on both sides of the mouse. For the direct injection, we injected 20  $\mu$ L of VEGF (at 5 mg/mL) using a Hamilton Neuros 25  $\mu$ L syringe adjusted for a penetration depth of 200  $\mu$ m. The muscle was exposed as described earlier and injected directly with the syringe. The incision was closed with staples as done with muscles treated with needles.

#### **RT-PCR analysis of plasmid VEGF delivery**

Animals treated with pSi nanoneedles with plasmid VEGF, direct injection of plasmid VEGF, or untreated were sacrificed at day 1, 3, 7, and 14 and the muscles were collected. Tissues were then stored in RNeasy lysis solution and kept at 4°C until further analysis. Tissues were then weighed out and added either 500 or 1000  $\mu$ L of Trizol depending on the weight. Tissues were then homogenized using a Pro Scientific PRO200 Bio-Gen Series homogenizer until tissue was fully digested. RNA was then extracted upon addition of chloroform and collection of the aqueous phase. RNA was then precipitated with isopropanol and washed with 75% ethanol and stored at -20°C in nuclease-free water. 0.5 to 1.0  $\mu$ g of RNA was retrotranscribed into cDNA using the iScript cDNA synthesis kit (Biorad). cDNA templates from each sample were mixed with TaqMan Fast Advanced Master Mix (Applied Biosystems), nuclease-free water, and TaqMan Gene Expression Assay (Human VEGFA and Mouse GAPDH, Applied Biosystems) for a total volume of 10  $\mu$ L. Samples were placed into MicroAmp Fast 96-well reaction plates and measured in triplicate using a StepOnePlus real time PCR system (Applied Biosystems).

#### **Live animal imaging and quantification**

pSi nanoneedles were loaded with DyLight 800 (Pierce Thermo Scientific) by incubating a concentrated solution (1  $\mu$ g/mL) of dye for five minutes and then removing the excess solution. Loaded pSi nanoneedles were applied on either the top of the skin or under the skin on the upper back. pSi nanoneedles were imaged using an IVIS 200 (Caliper Life Sciences) equipped with indocyanine green excitation and emission filters housed at the small imaging animal facility at MDACC. DyLight 800 loaded pSi nanoneedles were imaged at pre-determined

times to study the kinetics and distribution after delivery of dye over three days. Quantification of images and data was performed using the Living Image 4.1 software.

### **Intravital animal confocal microscopy**

The ability of pSi nanoneedles to deliver plasmid DNA was investigated by assessing the increase in the extent of neovascularization within the muscle using intravital confocal microscopy (ICM) after delivering plasmid VEGF-165 (pVEGF). Human pVEGF was a generous gift from Molecular Medicine International Centre for Genetic Engineering and Biotechnology (ICGEB, Trieste, Italy). 100 µg of pVEGF was loaded within pSi nanoneedles and carefully implanted on the right lumbar and gluteal muscle for 1 minute while the left side was left untouched as control. Fourteen days later, animals were prepared for ICM after removal of staples and injected with 40k FITC labeled dextran (Sigma Aldrich) and imaged for vasculature at the site of nanoneedle implantation. For ICM, an upright Nikon A1R laser scanning confocal microscope equipped with a resonance scanner, motorized and heated stage, and a Nikon long working distance 4x and 20x dry plan-apochromat objective were used. Images collected were analyzed using Nikon Elements (Nikon, USA).

### **H&E Histology**

Histological analysis for H&E and immunofluorescence for macrophages on muscle, skin, and ear was performed. Tissues were harvested and fixed in 10% buffered formalin overnight and then transferred to 70% ethanol prior to embedding into paraffin. Paraffin sections were then deparaffinized with xylene and re-hydrated with decreasing concentrations of ethanol followed by washings in water. For H&E sections staining occurred immediately after this step. For immunofluorescence, sections were transferred to pre-boiled sodium citrate buffer and microwaved for 20 minutes at low power to achieve antigen retrieval. Sections were then blocked for one hour followed by staining for macrophages using the anti-mouse F4/80 FITC (AbD Serotec) antibody for two hours. Sections were then stained with DAPI and coverslipped. Sections were imaged using a Nikon Eclipse 80i equipped with an Andor DL-604M (monochromatic) and Nikon DS-Fi1 (color) cameras and analyzed using the Nikon Elements software.

### **Transmission Electron Microscopy *in vivo***

Tissues were harvested and fixed in 0.1 M sodium cacodylate buffer containing 2.5% w/v glutaraldehyde and 3% w/v paraformaldehyde (Electron Microscopy Sciences) and stored 4°C until further processing. After fixation, the samples were washed in 0.1 M cacodylate buffer, postfixed with 1% w/v buffered osmium tetroxide for 2 hours, and stained en bloc with 1% w/v Millipore-filtered uranyl acetate. The samples were washed several times in water, then dehydrated in increasing concentrations of ethanol, infiltrated, and embedded in LX-112 medium. The samples were polymerized in a 60 °C oven for about 3 days. Ultrathin sections were cut in a Leica Ultracut microtome (Leica, Deerfield, IL), stained with uranyl acetate and lead citrate in a Leica EM Stainer, and examined in a JEM 1010 transmission electron microscope (JEOL, USA, Inc., Peabody, MA)

at an accelerating voltage of 80 kV. Digital images were obtained using AMT Imaging System (Advanced Microscopy Techniques Corp, Danvers, MA).

### Histological analysis of neovascularisation

Animals treated with pSi nanoneedles with plasmid VEGF, direct injection of plasmid VEGF, or untreated were perfused with 10% formalin and sacrificed at day 14. The muscle was collected at both the site of administration (VEGF) and the contralateral (Control) and stored overnight in 10% formalin and then transferred to 70% ethanol. Tissues were then further dehydrated and embedded in paraffin in two orientations: i) muscle was laid flat such that the site of administration was sectioned first near the top (i.e., transverse); ii) muscle was positioned such that we could examine the depth of penetration of the delivery (i.e., longitudinal). 4  $\mu$ m sections from each orientation were incubated at 60°C for 10 minutes followed by deparaffinization in xylene and rehydration through increasing concentrations of alcohol (100% to 50%) to distilled water. Sections were then blocked in 1% bovine serum albumin in PBS for one hour, followed by incubation with FITC  $\alpha$ -smooth muscle actin (Sigma Aldrich) or Alexa Fluor 594 isolectin B4 (Invitrogen) for two hours. Sections were then imaged using a Nikon Eclipse 80i equipped with an Andor monochrome camera, S Plan Fluor 20x Plan and Apo 40x objectives (Nikon). Images were then adjusted and exported using Nikon Elements.

### Statistical Analysis

Statistical analysis on all datasets was performed with Prism (GraphPad Software Inc., USA). All dataset with multiple timepoints (MTT, LDH) were analysed by two-way ANOVA followed by Bonferroni test to evaluate statistically significant differences with  $\alpha=0.05$ . GAPDH expression levels and intravital microscopy quantification data were analysed by one-way ANOVA, followed by Turkey post-test. All instances in which only two groups were compared employed two-tailed unpaired t-tests. \* $p<0.05$ , \*\* $p<0.01$ , \*\*\* $p<0.001$ .



## References

1. Smith, W. G. Analytic solutions for tapered column buckling. *Computers & Structures* **28**, 677–681 (1988).
2. Ji, J., Tay, F. E. H., Miao, J. & Iliescu, C. Microfabricated microneedle with porous tip for drug delivery. *J. Micromech. Microeng.* **16**, 958–964 (2006).
3. Duttagupta, S. P. & Fauchet, P. M. in *The Properties of Porous Silicon* (Canham, L. T.) 127 (EMIS Datareview).
4. Obataya, I., Nakamura, C., Han, S., Nakamura, N. & Miyake, J. Mechanical sensing of the penetration of various nanoneedles into a living cell using atomic force microscopy. *Biosensors and Bioelectronics* **20**, 1652–1655 (2005).
5. Chiappini, C., Liu, X., Fakhoury, J. R. & Ferrari, M. Biodegradable Porous Silicon Barcode Nanowires with Defined Geometry. *Adv. Funct. Mater.* **20**, 2231–2239 (2010).